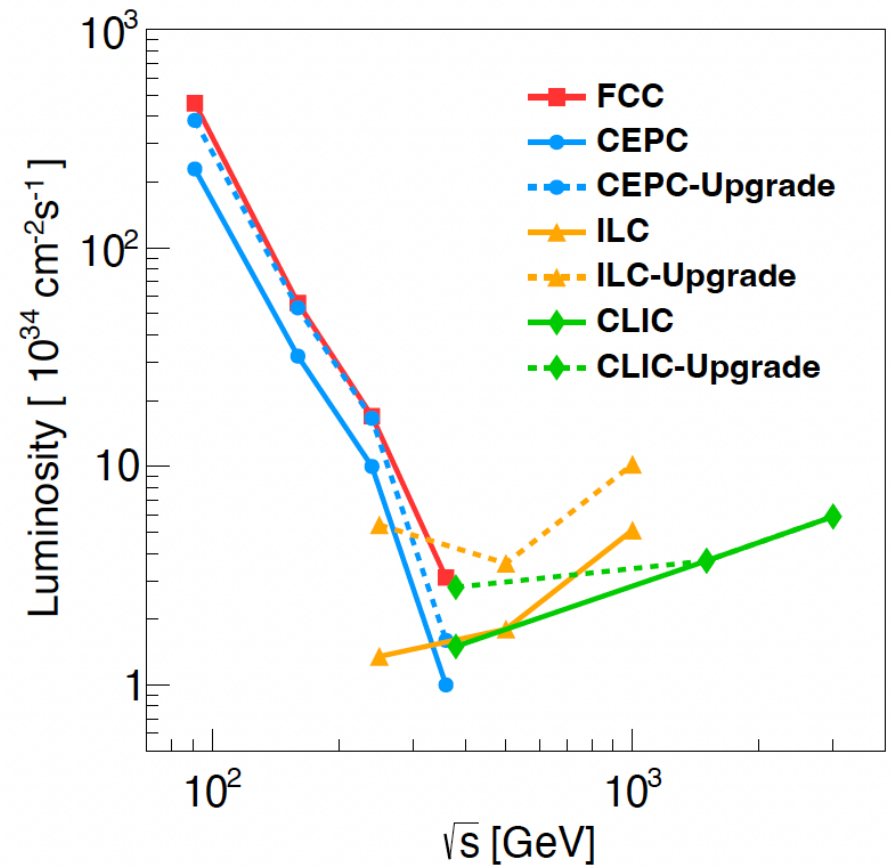
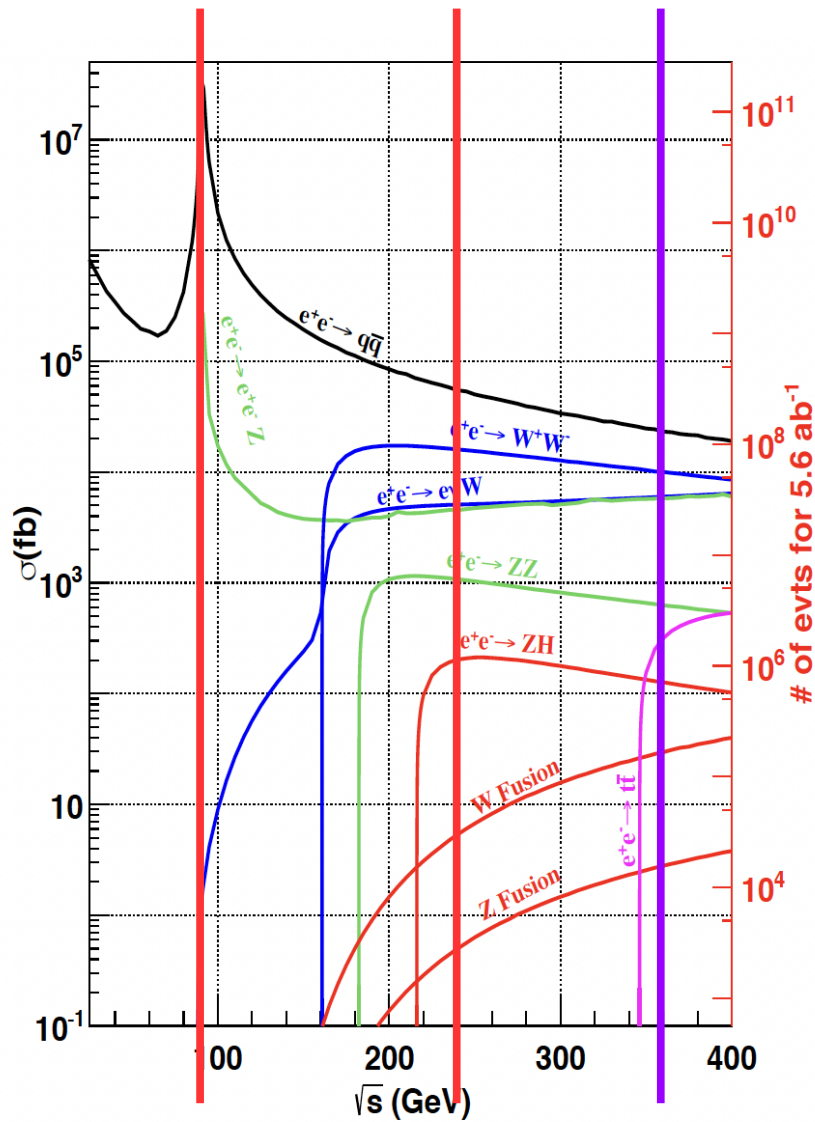




Physics Benchmark & Detector requirements

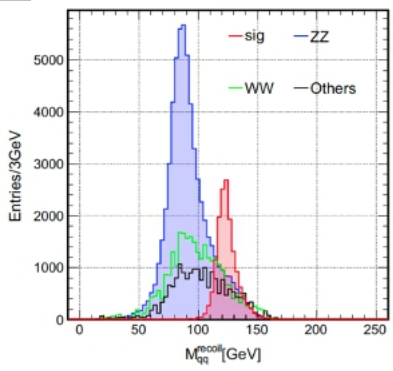
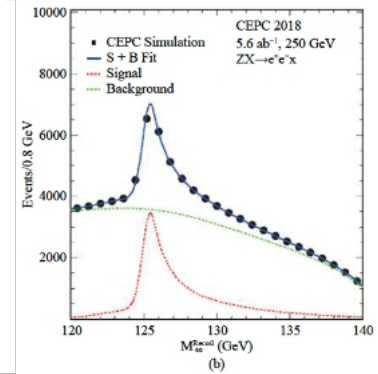
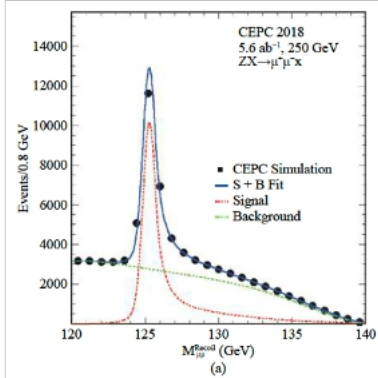
Manqi

Yields \sim Xsec * Lumi * Time



- 4 Million Higgs (10 years)
- ~ 1 Giga W (1 year) + 4 Tera Z (2 years)
- Upgradable: Top factory (500 k ttbar)

Physics study: 2023



Chinese Physics C Vol. 43, No. 4 (2019) 043002

Precision Higgs physics at the CEPC*

Fenfen An(安芬芬)^{4,23} Yu Bai(白羽)⁶ Chunhui Chen(陈春晖)²³ Xin Chen(陈新)⁵ Zhenxing Chen(陈振兴)⁸ Joao Guimaraes da Costa¹ Zhenwei Cui(崔振威)³ Yaquan Fang(方亚泉)^{4,6,34,35} Chengdong Fu(付成栋)¹ Jun Gao(高俊)²³ Yanyan Gao(高艳彦)²² Yuanming Gao(高原宁)⁷ Shaofeng Ge(葛韶锋)^{13,29} Jiayin Gu(顾嘉茵)^{13,29} Fangyi Guo(郭方懿)^{4,4} Jun Guo(郭军)¹⁹ Tao Han(韩涛)³¹ Shuang Han(韩爽)⁴ Hongjian He(何红建)^{11,19} Xianke He(何显柯)¹⁶ Xiaogang He(何小刚)^{11,16,20} Jifeng Hu(胡耀峰)¹⁶ Shih-Chieh Hsu(徐士杰)¹² Shan Jin(金山)⁸ Maoqiang Jing(荆茂强)^{4,5} Susmita JyotiShamti³³ Ryuta Kinoshita⁴ Chia-Ming Kuo(郭家铭)¹¹ Peizhuo Lai(赖培筑)³ Boyang Li(李博扬)³ Congqiao Li(李聪乔)³ Gang Li(李刚)^{4,34,35} Haifeng Li(李海峰)¹² Liang Li(李亮)¹⁹ Shu Li(李数)^{11,19} Tong Li(李通)¹² Qiang Li(李强)³ Hao Liang(梁浩)^{4,6} Zhijun Liang(梁志均)⁴ Libo Liao(廖立波)⁴ Bo Liu(刘波)^{4,23} Jianbei Lin(刘建北)³ Tao Liu(刘涛)¹⁴ Zhen Liu(刘真)^{28,36,6} Xinchou Lou(娄辛丑)^{4,43,14} Lianliang Ma(马连良)¹² Bruce Mellado^{13,18} Xin Mo(莫欣)⁴ Mila Pandurovic¹⁶ Jianming Qian(钱剑明)^{4,23} Zhaonai Qian(钱卓妮)¹⁹ Nikolaos Rempotis²² Manqi Ruan(阮曼奇)^{4,6} Alex Schry³² Lianyou Shan(单连友)⁴ Jingyuan Shi(史静远)⁴ Xin Shi(史欣)⁴ Shufang Su(苏淑芳)^{7,7} Dayong Wang(王大勇)³ Jun Wang(王隼)⁴ Liantao Wang(王连涛)^{7,7} Yifang Wang(王贻芳)^{4,6} Yuqian Wei(魏或琦)⁴ Yue Xu(许悦)³ Haijun Yang(杨海军)^{30,31} Ying Yang(杨迎)⁴ Weiming Yao(姚伟明)⁷ Dan Yu(于丹)⁴ Kaiji Zhang(张凯冀)^{4,49} Zhaoru Zhang(张照茹)⁴ Mingrui Zhao(赵明锐)⁷ Xiaoguo Zhao(赵祥虎)⁴ Ning Zhou(周宁)¹⁹

White papers + ~300 Journal/AxXiv citables

Qingdao 266237, China
¹PRISMA Cluster of Excellence & Mainz Institute of Theoretical Physics, Johannes Gutenberg-Universität Mainz, Mainz 55128, Germany
²Department of Physics, Hong Kong University of Science and Technology, Hong Kong
³Kevin IPMU (WPI), UTIAS, The University of Tokyo, Kashiwa, Chiba 277-8583, Japan
⁴Vincas Institute of Nuclear Sciences, University of Belgrade, Belgrade 11000, Serbia
⁵School of Physics and Institute for Collider Particle Physics, University of the Witwatersrand, Johannesburg 2050, South Africa

Received 9 November 2018; Revised 21 January 2019; Published online 4 March 2019
 * Supported by the National Key Program for S&T Research and Development (2016YFA040400); CAS Center for Excellence in Particle Physics; Yifang Wang's Science Studio of the Ten Thousand Talents Project; the CAS-SAFEA International Partnership Program for Creative Research Teams (H21518183); BHEP Innovation Grant (Y454517072); Key Research Program of Frontier Sciences, CAS (SQZDY-SSW-SL3002); Chinese Academy of Science Special Grant for Large Scientific Project (113111KY5B20170005); the National Natural Science Foundation of China(11675203); the Hundred Talent Programs of Chinese Academy of Science (Y3151540U1); the National 1000 Talents Program of China; Feizi Research Alliance, LLC (DE-AC02-07CH11359); the NSF(PHY1610074); by the Maryland Center for Fundamental Physics (MCFP); Tsinghua University Initiative Scientific Research Program; and the Beijing Municipal Science and Technology Commission project(Z211100004218003)

1) E-mail: fangyi@dep.ac.cn
 2) E-mail: jiang@ust.hk
 3) E-mail: li.gang@mail.ust.hk
 4) E-mail: zhanghs@impu.edu
 5) E-mail: qianj@ust.hk
 6) E-mail: manqi.ruan@dep.ac.cn
 7) E-mail: liantao@ucicago.edu
 8) E-mail: zhangk1@dep.ac.cn

Content from this work may be used under the terms of the Creative Commons Attribution 3.0 licence. Any further distribution of this work must maintain attribution to the author(s) and the title of the work, journal citation and DOI. Article funded by SCOAP³ and published under licence by Chinese Physical Society and the Institute of High Energy Physics of the Chinese Academy of Sciences and the Institute of Modern Physics of the Chinese Academy of Sciences and IOP Publishing Ltd

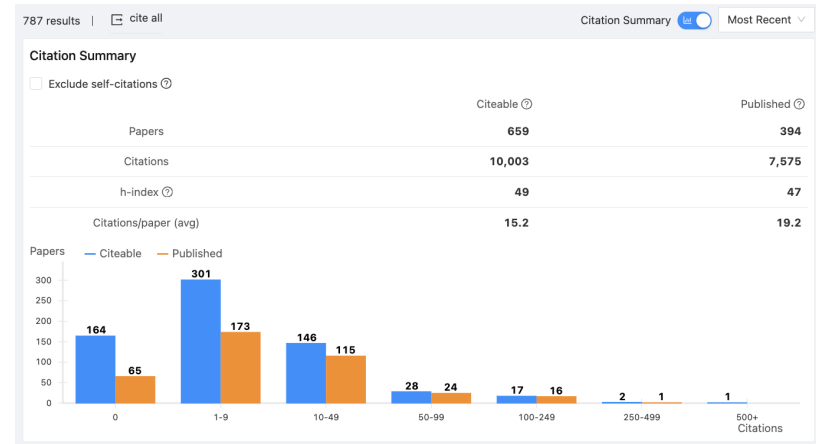


Table 2.1: Precision of the main parameters of interests and observables at the CEPC, from Ref. [1] and the references therein, where the results of Higgs are estimated with a data sample of 20 ab⁻¹. The HL-LHC projections of 3000 fb⁻¹ data are used for comparison. [2]

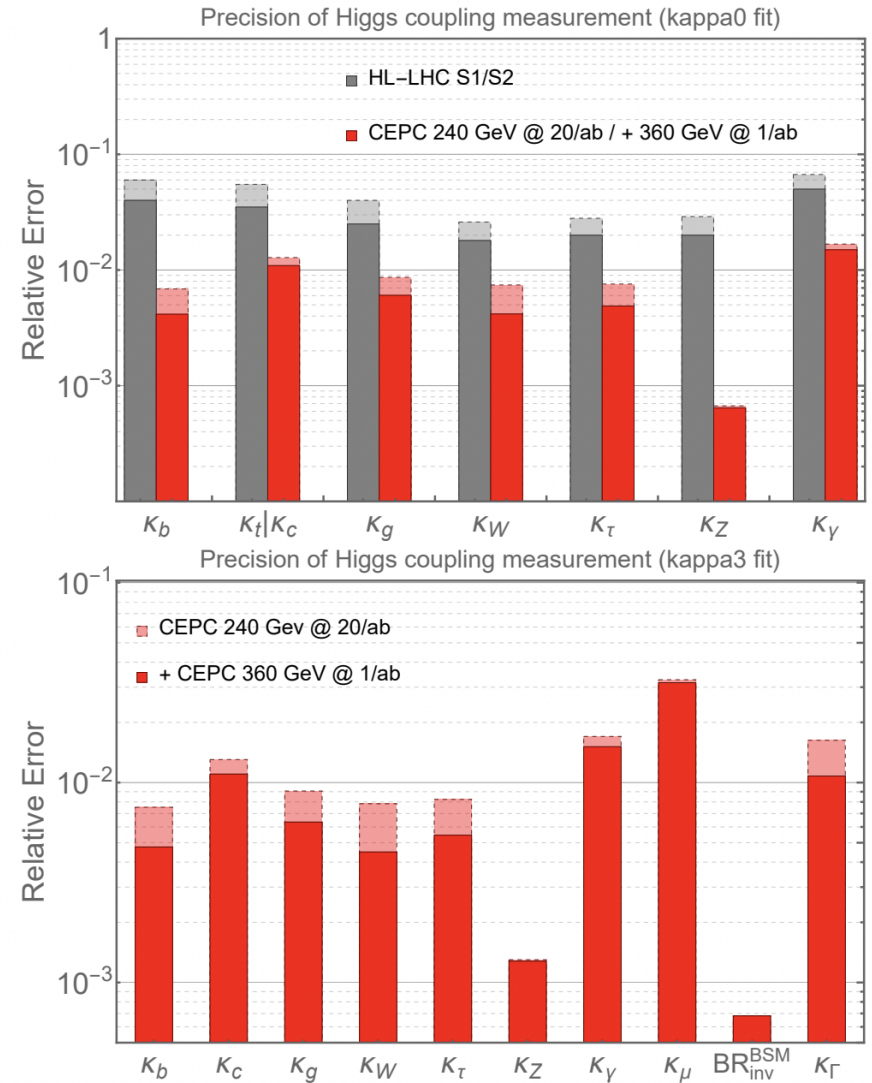
Observable	Higgs		W, Z and top		
	HL-LHC projections	CEPC precision	Observable	Current precision	CEPC precision
M_H	20 MeV	3 MeV	M_W	9 MeV	0.5 MeV
Γ_H	20%	1.7%	Γ_W	49 MeV	2 MeV
$\sigma(ZH)$	4.2%	0.26%	M_{top}	760 MeV	$\mathcal{O}(10)$ MeV
$B(H \rightarrow bb)$	4.4%	0.14%	M_Z	2.1 MeV	0.1 MeV
$B(H \rightarrow cc)$	-	2.0%	Γ_Z	2.3 MeV	0.025 MeV
$B(H \rightarrow gg)$	-	0.81%	R_b	3×10^{-3}	2×10^{-4}
$B(H \rightarrow WW^*)$	2.8%	0.53%	R_c	1.7×10^{-2}	1×10^{-3}
$B(H \rightarrow ZZ^*)$	2.9%	4.2%	R_μ	2×10^{-3}	1×10^{-4}
$B(H \rightarrow \tau^+\tau^-)$	2.9%	0.42%	R_τ	1.7×10^{-2}	1×10^{-4}
$B(H \rightarrow \gamma\gamma)$	2.6%	3.0%	A_μ	1.5×10^{-2}	3.5×10^{-5}
$B(H \rightarrow \mu^+\mu^-)$	8.2%	6.4%	A_τ	4.3×10^{-3}	7×10^{-5}
$B(H \rightarrow Z\gamma)$	20%	8.5%	A_b	2×10^{-2}	2×10^{-4}
$B(\text{upper}(H \rightarrow \text{inv.}))$	2.5%	0.07%	N_ν	2.5×10^{-3}	2×10^{-4}

Scientific Significance quantified by CEPC physics studies, via full simulation/phenomenology studies:

- Higgs: Precisions exceed HL-LHC ~ 1 order of magnitude.
- EW: Precision improved from current limit by 1-2 orders.
- Flavor Physics, sensitive to NP of 10 TeV or even higher.
- Sensitive to varies of NP signal.
- ...

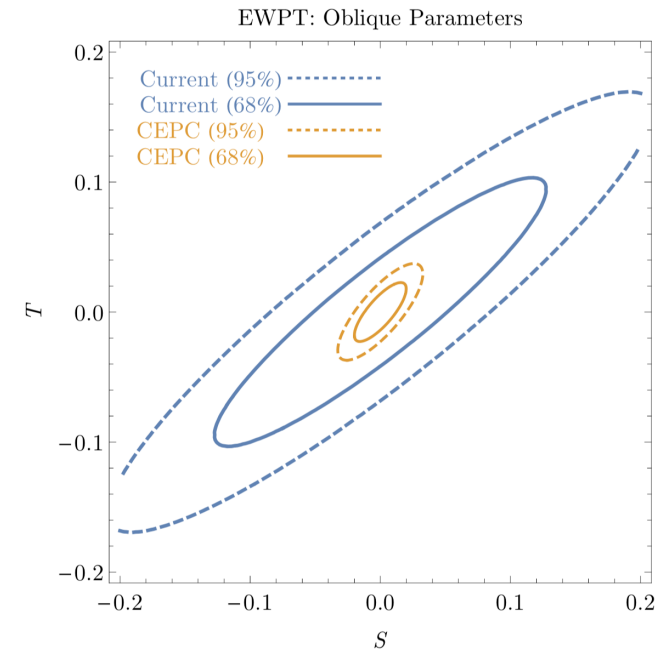
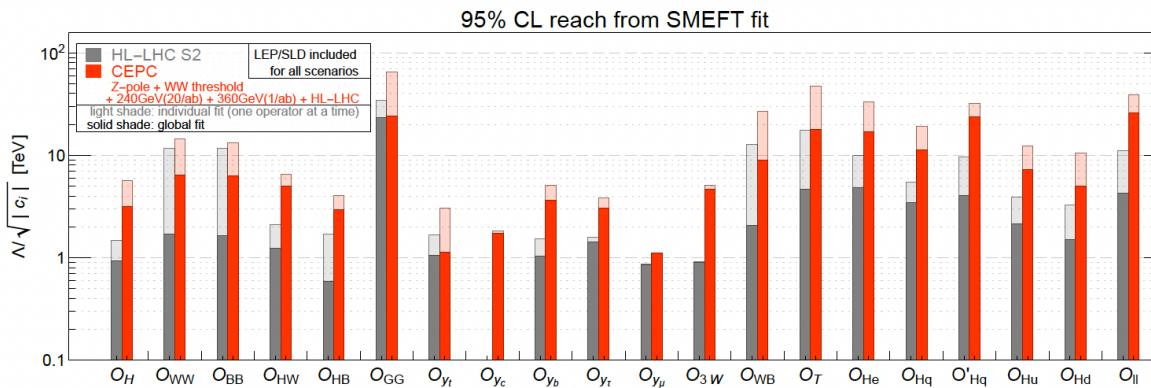
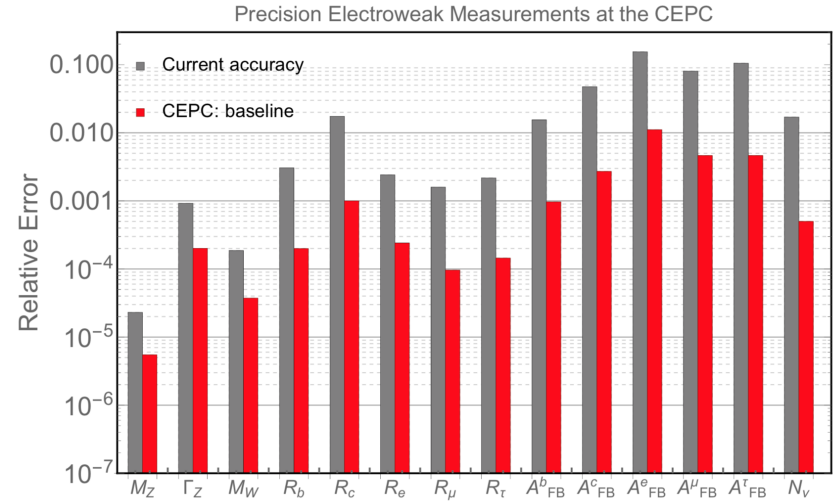
Physics reach via Higgs at CEPC

	240 GeV, 20 ab^{-1}		360 GeV, 1 ab^{-1}		
	ZH	$\nu\nu\text{H}$	ZH	$\nu\nu\text{H}$	eeH
inclusive	0.26%		1.40%	\	\
$\text{H} \rightarrow \text{bb}$	0.14%	1.59%	0.90%	1.10%	4.30%
$\text{H} \rightarrow \text{cc}$	2.02%		8.80%	16%	20%
$\text{H} \rightarrow \text{gg}$	0.81%		3.40%	4.50%	12%
$\text{H} \rightarrow \text{WW}$	0.53%		2.80%	4.40%	6.50%
$\text{H} \rightarrow \text{ZZ}$	4.17%		20%	21%	
$\text{H} \rightarrow \tau\tau$	0.42%		2.10%	4.20%	7.50%
$\text{H} \rightarrow \gamma\gamma$	3.02%		11%	16%	
$\text{H} \rightarrow \mu\mu$	6.36%		41%	57%	
$\text{H} \rightarrow \text{Z}\gamma$	8.50%		35%		
$\text{Br}_{\text{upper}}(\text{H} \rightarrow \text{inv.})$	0.07%				
Γ_{H}	1.65%		1.10%		



EW measurements & SMEFT

Observable	current precision	CEPC precision (Stat. Unc.)	CEPC runs	main systematic
Δm_Z	2.1 MeV [37–41]	0.1 MeV (0.005 MeV)	Z threshold	E_{beam}
$\Delta \Gamma_Z$	2.3 MeV [37–41]	0.025 MeV (0.005 MeV)	Z threshold	E_{beam}
Δm_W	9 MeV [42–46]	0.5 MeV (0.35 MeV)	WW threshold	E_{beam}
$\Delta \Gamma_W$	49 MeV [46–49]	2.0 MeV (1.8 MeV)	WW threshold	E_{beam}
Δm_t	0.76 GeV [50]	$\mathcal{O}(10)$ MeV ^a	$t\bar{t}$ threshold	
ΔA_e	4.9×10^{-3} [37, 51–55]	1.5×10^{-5} (1.5×10^{-5})	Z pole ($Z \rightarrow \tau\tau$)	Stat. Unc.
ΔA_μ	0.015 [37, 53]	3.5×10^{-5} (3.0×10^{-5})	Z pole ($Z \rightarrow \mu\mu$)	point-to-point Unc.
ΔA_τ	4.3×10^{-3} [37, 51–55]	7.0×10^{-5} (1.2×10^{-5})	Z pole ($Z \rightarrow \tau\tau$)	tau decay model
ΔA_b	0.02 [37, 56]	20×10^{-5} (3×10^{-5})	Z pole	QCD effects
ΔA_c	0.027 [37, 56]	30×10^{-5} (6×10^{-5})	Z pole	QCD effects
$\Delta \sigma_{had}$	37 pb [37–41]	2 pb (0.05 pb)	Z pole	luminosity
δR_b^0	0.003 [37, 57–61]	0.0002 (5×10^{-6})	Z pole	gluon splitting
δR_c^0	0.017 [37, 57, 62–65]	0.001 (2×10^{-5})	Z pole	gluon splitting
δR_e^0	0.0012 [37–41]	2×10^{-4} (3×10^{-6})	Z pole	E_{beam} and t channel
δR_μ^0	0.002 [37–41]	1×10^{-4} (3×10^{-6})	Z pole	E_{beam}
δR_τ^0	0.017 [37–41]	1×10^{-4} (3×10^{-6})	Z pole	E_{beam}
δN_ν	0.0025 [37, 66]	2×10^{-4} (3×10^{-5})	ZH run ($\nu\nu\gamma$)	Calo energy scale



Flavor Physics White paper

Flavor Physics at CEPC: a General Perspective

Contents

1	Introduction	2
2	Description of the CEPC Facility	6
2.1	Key Collider Features for Flavor Physics	6
2.2	Key Detector Features for Flavor Physics	7
2.3	Simulation Method	14
3	Charged Current Semileptonic and Leptonic b -Flavored Hadron Decays	16
4	Rare/Penguin and Forbidden b -Flavored Hadron Decays	22
4.1	Dilepton Modes	24
4.2	Neutrino Modes	26
4.3	Radiative Modes	28
5	CP Asymmetry in b -Flavored Hadron Decays	29
6	Global Symmetry Tests in Z and b -Flavored Hadron Decays	34
7	Charm and Strange Physics	37
7.1	Null Tests with Rare Charm Decays	38
8	τ Physics	38
8.1	LFV τ Decays	39
8.2	LFU Tests in τ Decays	40
8.3	Hadronic τ Decays and Other Opportunities	42
8.4	CPV in Hadronic τ Decays	43
9	Exclusive Hadronic Z Decays	44
10	Flavor Physics beyond Z Pole	45
10.1	$ V_{cb} $ and W Decays	46
10.2	Higgs Exotic and FCNC	47
10.3	Top FCNC	49
11	Spectroscopy and Exotics	50
12	Light BSM States from Heavy Flavors	55
12.1	Lepton Sector	55
12.2	Quark Sector	57
13	Summary and Outlook	58

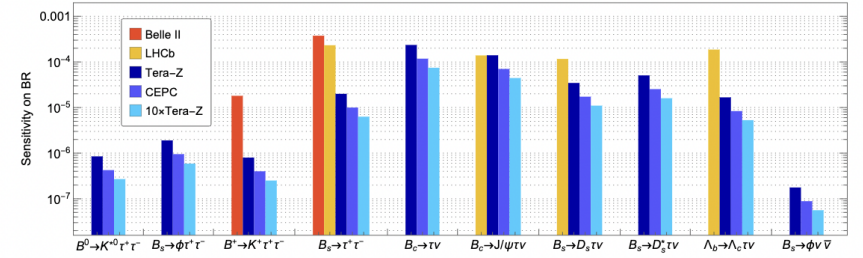


Figure 18: Projected sensitivities of measuring the $b \rightarrow s\tau\tau$ [70], $b \rightarrow s\nu\bar{\nu}$ [34] and $b \rightarrow c\tau\nu$ [35, 62] transitions at the Z pole. The sensitivities at Belle II @ 50 ab^{-1} [6] and LHCb Upgrade II [17, 71] have also been provided as a reference. Note, the LHCb sensitivities are generated by combining the analyses of $\tau^+ \rightarrow \pi^+\pi^-\pi^0\nu$ and $\tau \rightarrow \mu\nu\bar{\nu}$. This plot is adapted from [35].

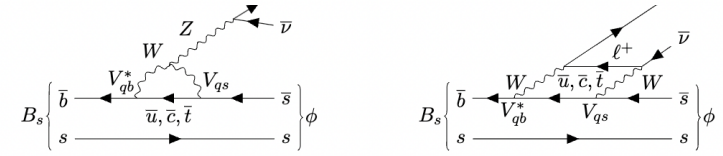


Figure 21: Illustrative Feynman diagrams for the $B_s \rightarrow \phi\nu\bar{\nu}$ transitions in the SM. **LEFT:** EW penguin diagram. **RIGHT:** EW box diagram.

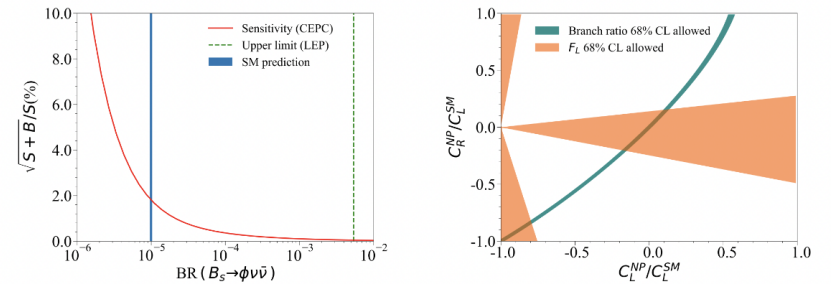


Figure 22: **LEFT:** Relative precision for measuring the signal strength of $B_s \rightarrow \phi\nu\bar{\nu}$ at Tera-Z, as a function of its BR. **RIGHT:** Constraints on the LEFT coefficients $C_L^{\text{NP}} \equiv C_L - C_L^{\text{SM}}$ and C_R with the measurements of the overall $B_s \rightarrow \phi\nu\bar{\nu}$ decay rate (green band) and the ϕ polarization F_L (orange regions). These plots are taken from [34].

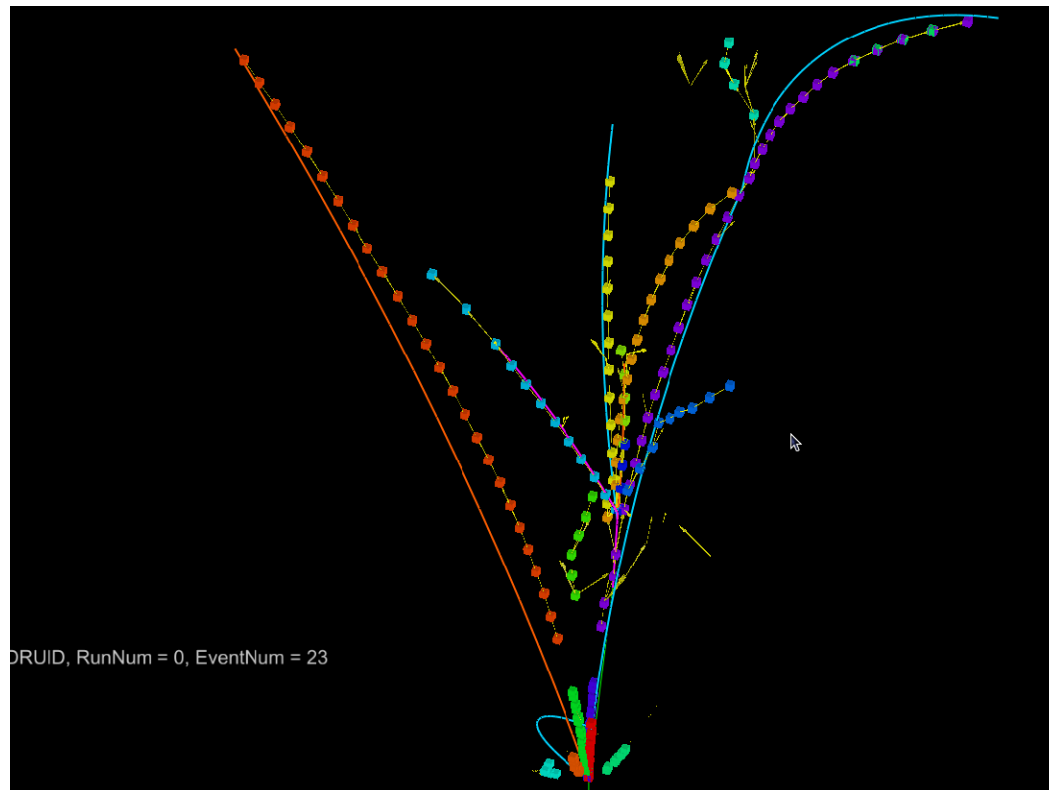
Physics Benchmarks

	Processes @ c.m.s.	Domain	Total Det. Performance	Sub-D
H->ss/cc/sb	vvH @ 240 GeV	Higgs	PFA + JOI (Jet origin id)	All sub-D, especially VTX
H->inv	qqH	Higgs/NP	PFA	All
Vcb	WW@ 240/160 GeV	Flavor	JOI + Particle (lepton) id	All
W fusion Xsec	vvH @ 360 GeV	Higgs	PFA + JOI	All
α_s	Z->tautau @ 91.2 GeV	QCD	PFA: Tau & Tau final state id	ECAL + Tracker material
B->DK	91.2 GeV	Flavor	PFA + Particle (Kaon) id	All, especially Tracker & ToF
Weak mixing angle	Z	EW	JOI	All
Higgs recoil	llH	Higgs	Leptons id, track dP/P	Tracker, All
H->bb, cc, gg	vvH	Higgs	PFA + JOI	All
	qqH	Higgs	PFA + JOI + Color Singlet id	All
H->di muon	qqH	Higgs	PFA, Leptons id	Calo, All
H->di photon	qqH	Higgs	PFA, Photons id	ECAL, All
W mass & Width	WW@160 GeV	EW	Beam energy	NAN
Top mass & Width	ttbar@360 GeV	EW	Beam energy	NAN
Bs->vvPhi	Z	Flavor	Object in jets; MET	All
Bc->tauv	Z	Flavor	-	All
B0->2 pi0	Z	Flavor	Particle/pi-0 in jets	ECAL

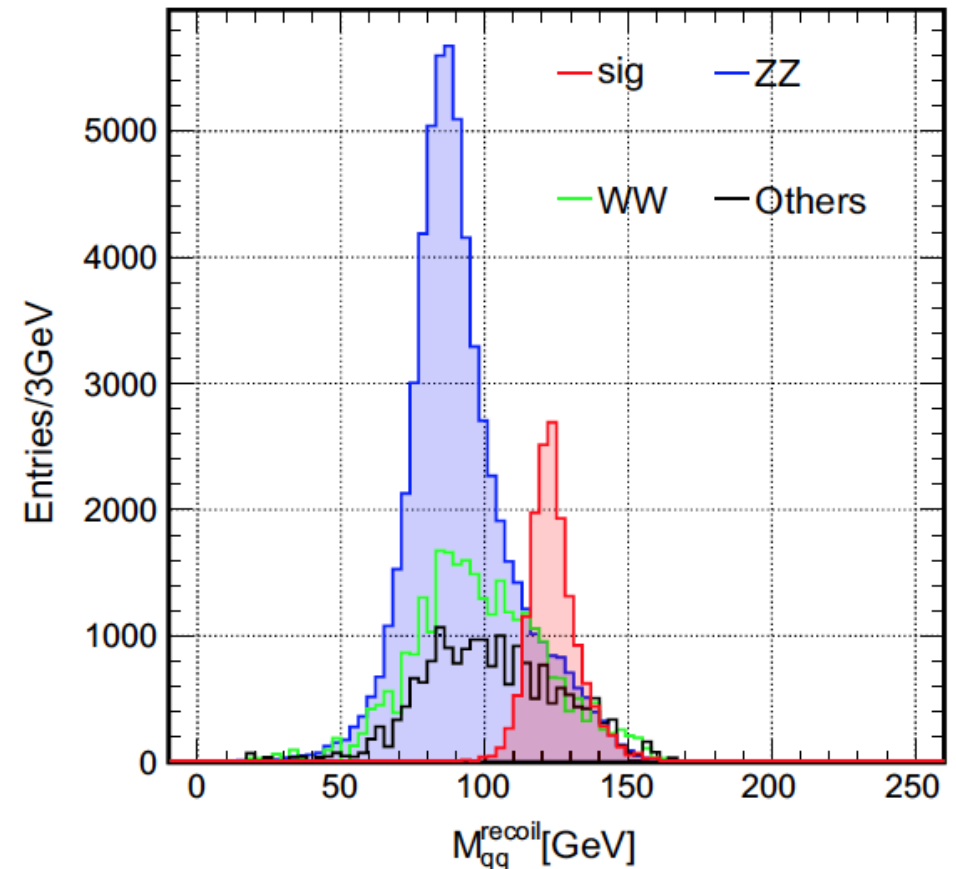
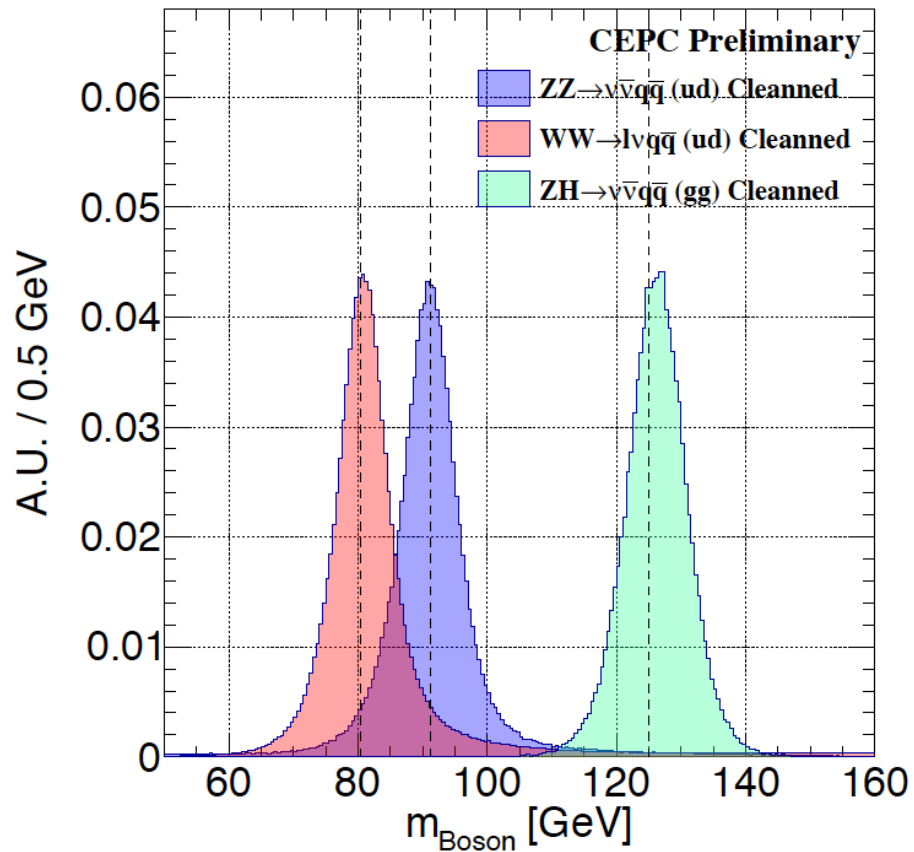
Performance requirements

- A clear separation of the final state particles: Identification of Physics Objects, and Improving the E/P resolution for composited objects, especially jets
 - Leptons, especially these inside jets
 - Composited objects:
 - Two/three body objects: Pi-0, K-short, Lambda, Phi, Tau, D meson...
 - More bodies: Tau & Jets
 - **PFA: pursuing 1-1 correspondence.**
 - BMR (Boson Mass Resolution): mass resolution of Hadronic decayed Higgs/Z/W
BMR < 4% for Higgs measurements
 - Much demanding for Flavor Physics/New Physics Hunting
- **Pid:**
 - Pion & Kaon separation > 3 σ
 - Identify species of all charged final state particles: isolated and **in jet**...
- **Jet origin id:** Flavor Tagging & Charge Reconstruction, s-jet id, gluon jet id, etc
- Intrinsic accuracies: momentum, energy, VTX positions...

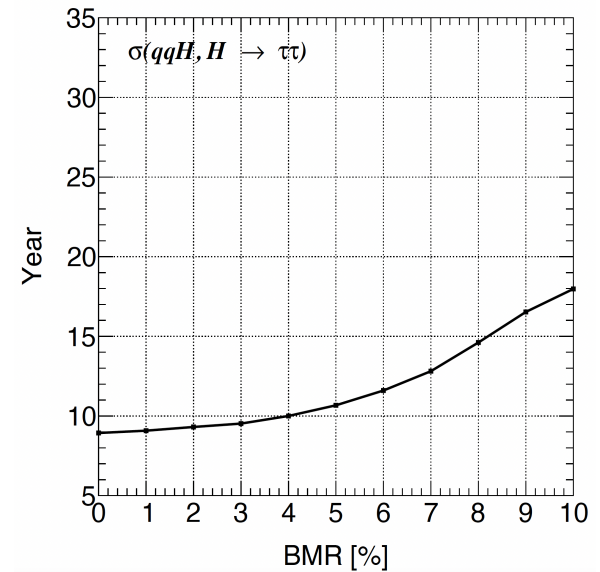
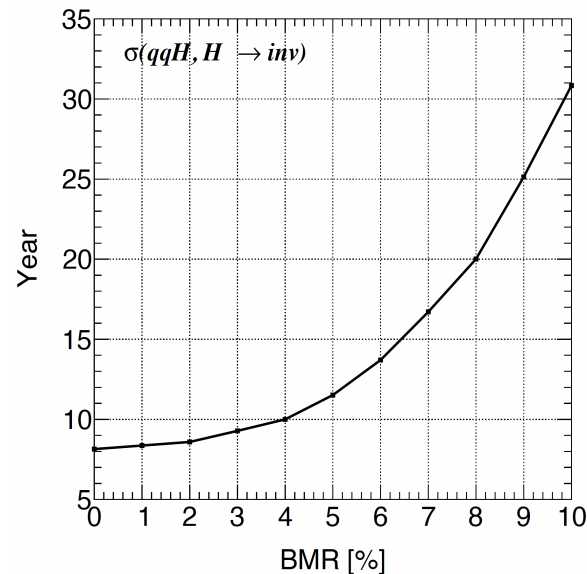
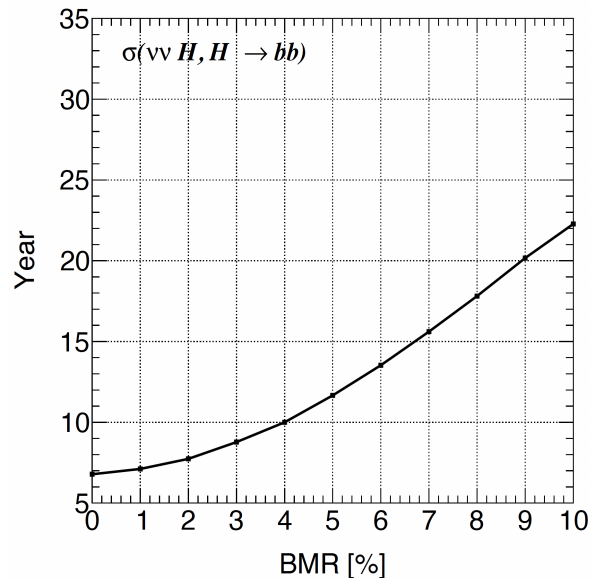
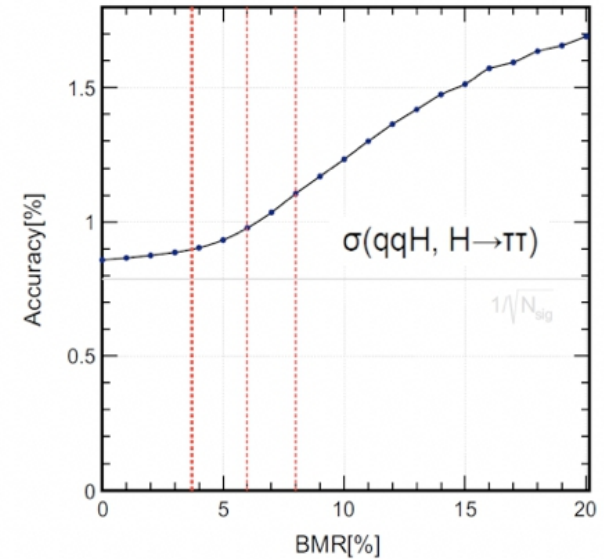
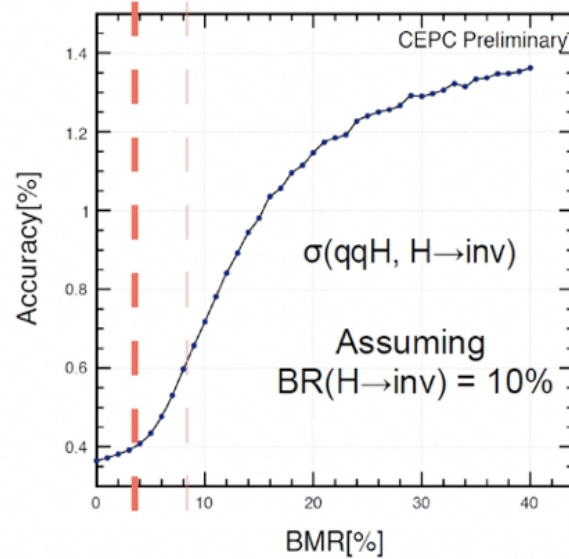
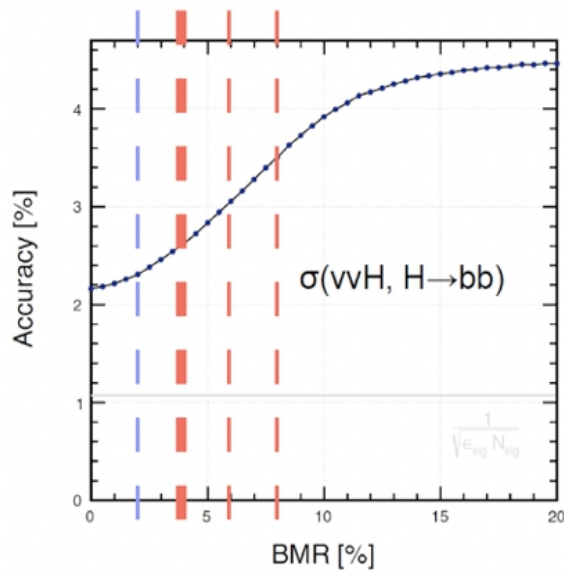
PFA



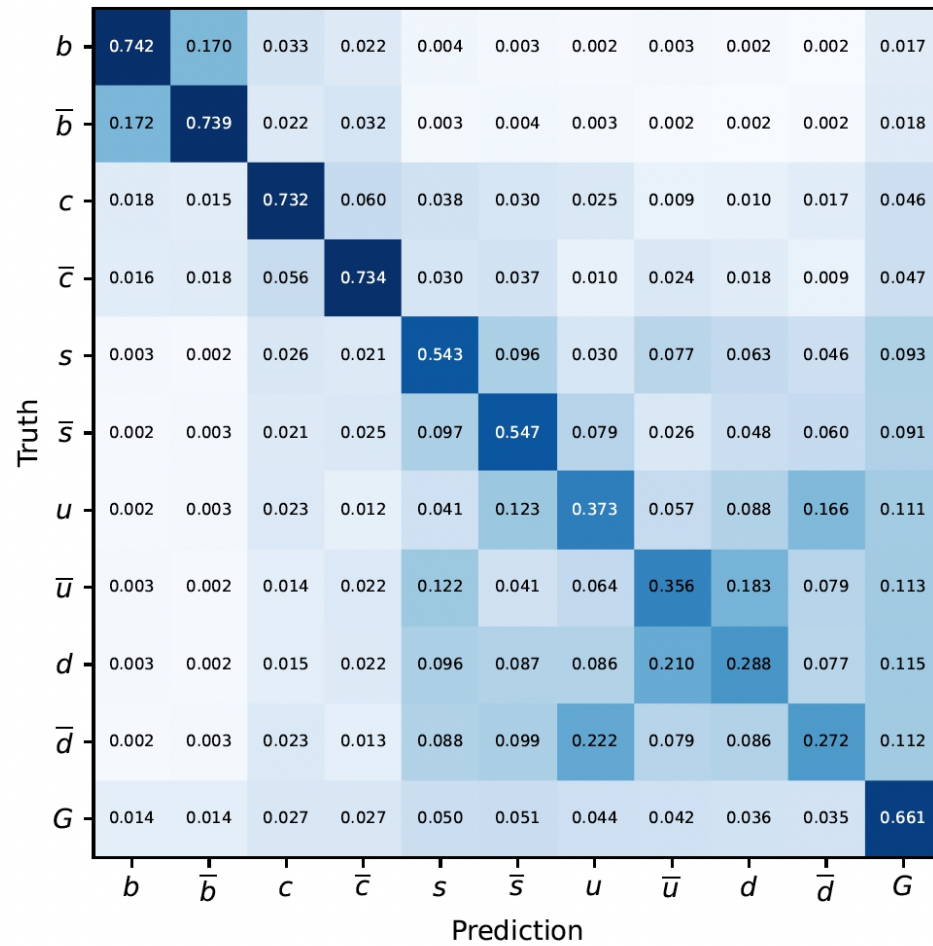
Boson Mass Resolution: Key Per. Para



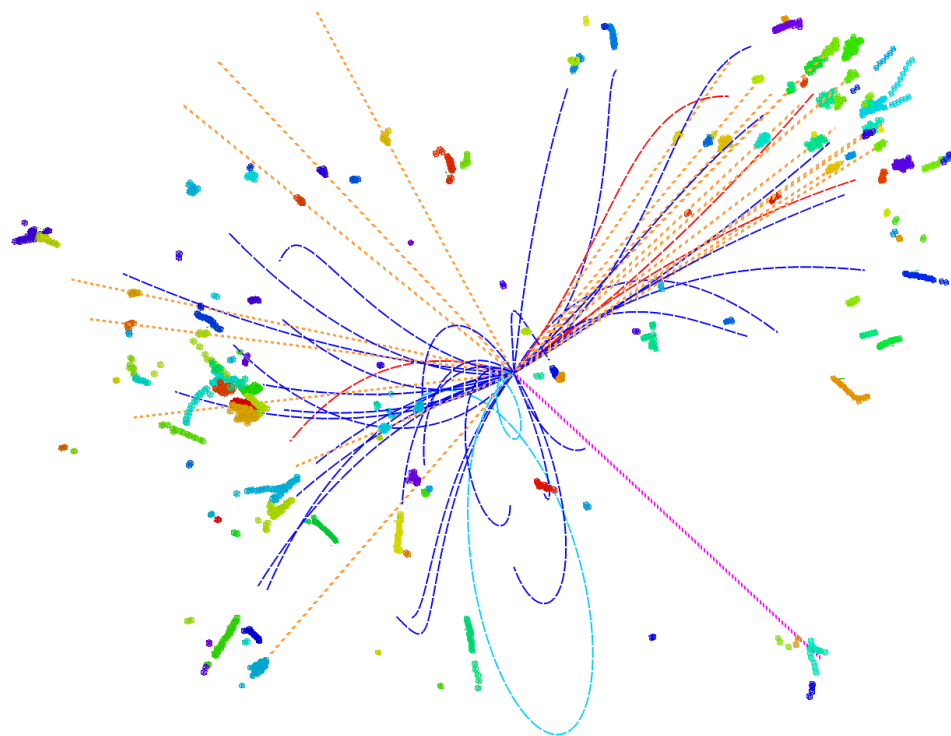
BMR: impact on critical measurements



Jet origin id



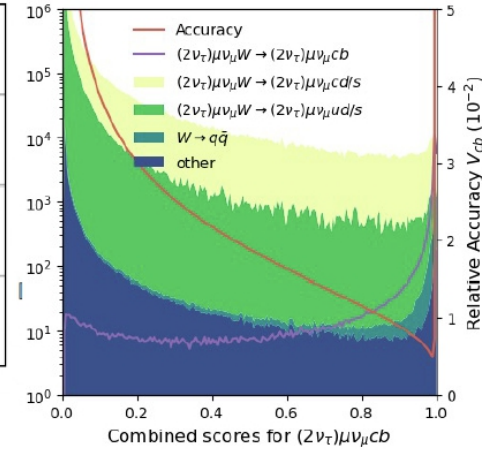
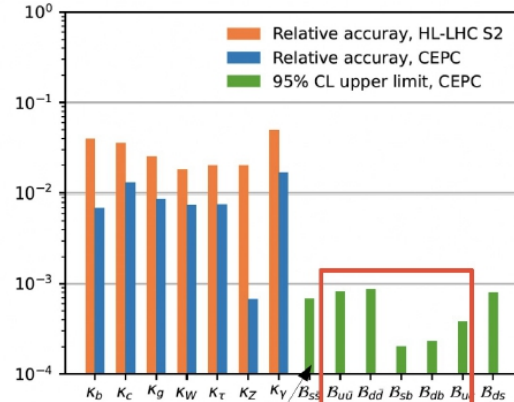
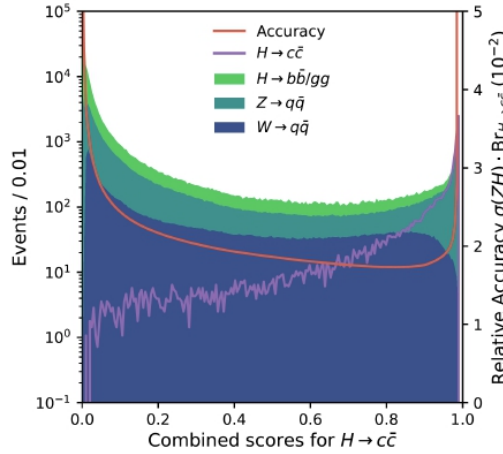
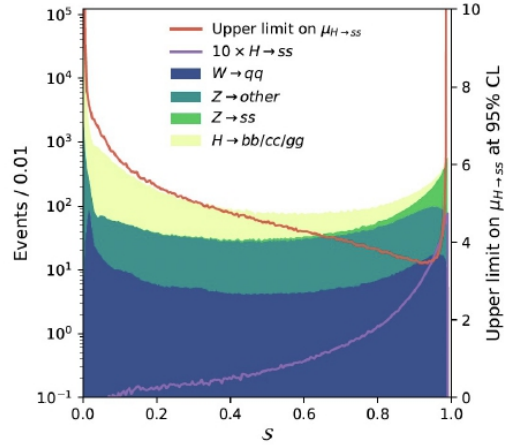
Jet origin id



b	0.742	0.170	0.033	0.022	0.004	0.003	0.002	0.003	0.002	0.002	0.017
\bar{b}	0.172	0.739	0.022	0.032	0.003	0.004	0.003	0.002	0.002	0.002	0.018
c	0.018	0.015	0.732	0.060	0.038	0.030	0.025	0.009	0.010	0.017	0.046
\bar{c}	0.016	0.018	0.056	0.734	0.030	0.037	0.010	0.024	0.018	0.009	0.047
s	0.003	0.002	0.026	0.021	0.543	0.096	0.030	0.077	0.063	0.046	0.093
\bar{s}	0.002	0.003	0.021	0.025	0.097	0.547	0.079	0.026	0.048	0.060	0.091
u	0.002	0.003	0.023	0.012	0.041	0.123	0.373	0.057	0.088	0.166	0.111
\bar{u}	0.003	0.002	0.014	0.022	0.122	0.041	0.064	0.356	0.183	0.079	0.113
d	0.003	0.002	0.015	0.022	0.096	0.087	0.086	0.210	0.288	0.077	0.115
\bar{d}	0.002	0.003	0.023	0.013	0.088	0.099	0.222	0.079	0.086	0.272	0.112
G	0.014	0.014	0.027	0.027	0.050	0.051	0.044	0.042	0.036	0.035	0.661
	b	\bar{b}	c	\bar{c}	s	\bar{s}	u	\bar{u}	d	\bar{d}	G

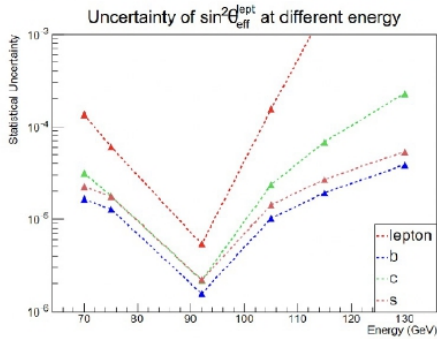
- **Jet origin identification: 11 categories (5 quarks + 5 anti quarks + gluon)**
 - Jet Flavor Tagging + Jet Charge measurements + s-tagging + gluon tagging...
- Full Simulated vvH , Higgs to two jets sample at CEPC baseline configuration: CEPC-v4 detector, reconstructed with **Arbor + ParticleNet (Deep Learning Tech.)**
- 1 Million samples each, 60/20/20% for training, validation & test

Impact on Physics

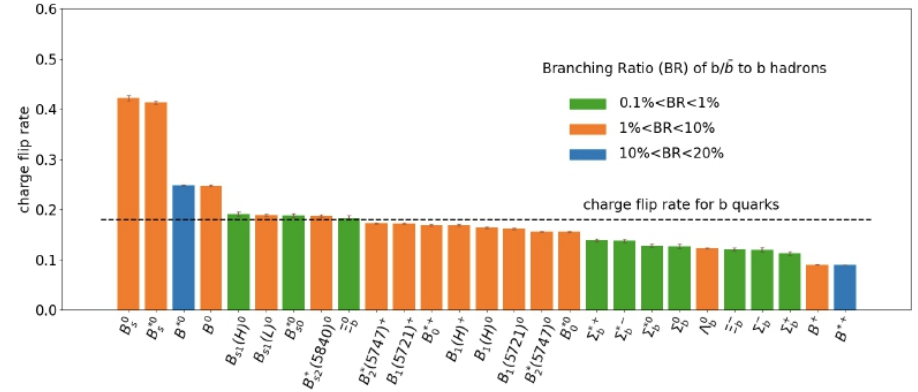


Improved by ~ 3 times
 Improved by 1-2 orders of magnitudes
 Presumably... firstly quantified

Expected statistical uncertainties on $\sin^2 \theta_{eff}^l$ measurement.
 (Using one-month data collection, $\sim 4e12/24$ Z events at Z pole)



\sqrt{s}	b	c	s
70	1.6×10^{-5}	3.2×10^{-5}	2.2×10^{-5}
75	1.3×10^{-5}	1.8×10^{-5}	1.8×10^{-5}
92	1.6×10^{-6}	2.2×10^{-6}	2.2×10^{-6}
105	1.0×10^{-5}	2.4×10^{-5}	1.4×10^{-5}
115	1.9×10^{-5}	6.8×10^{-5}	2.7×10^{-5}
130	3.9×10^{-5}	2.3×10^{-4}	5.4×10^{-5}

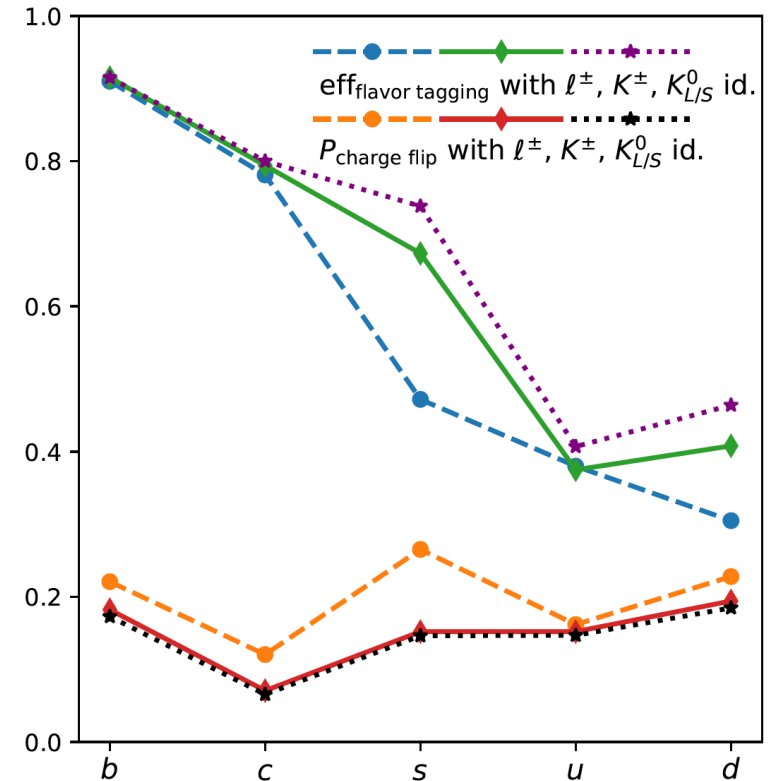
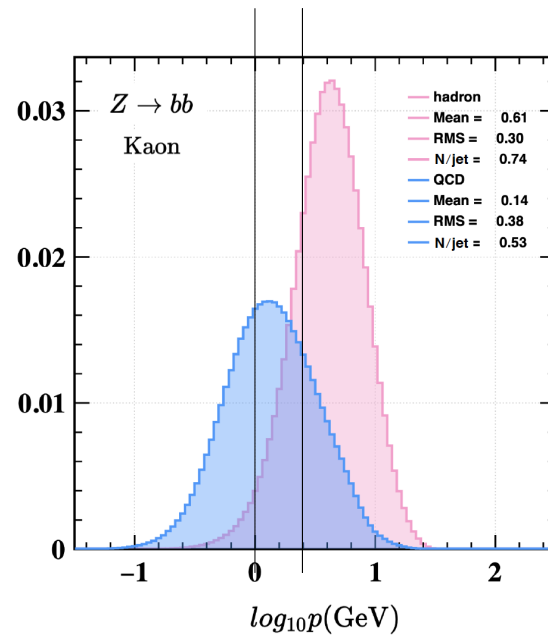
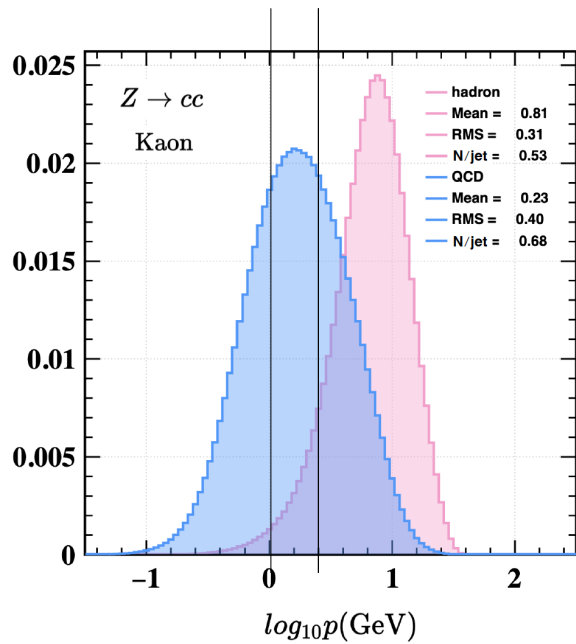


Particle identification

1. Kaon id

2. all species... + inside jets

Momentum spectrum of Kaon...

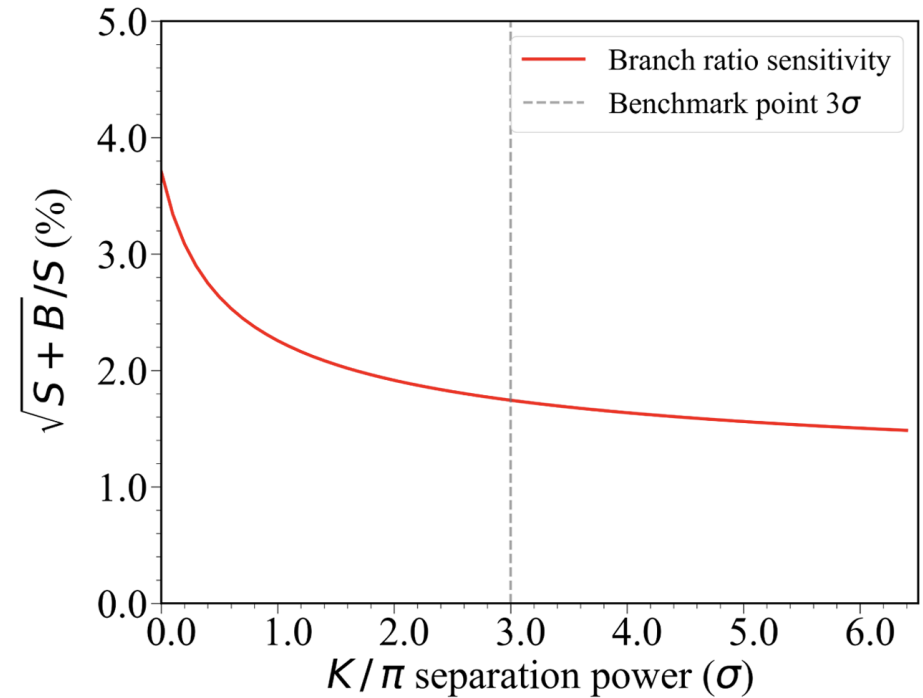
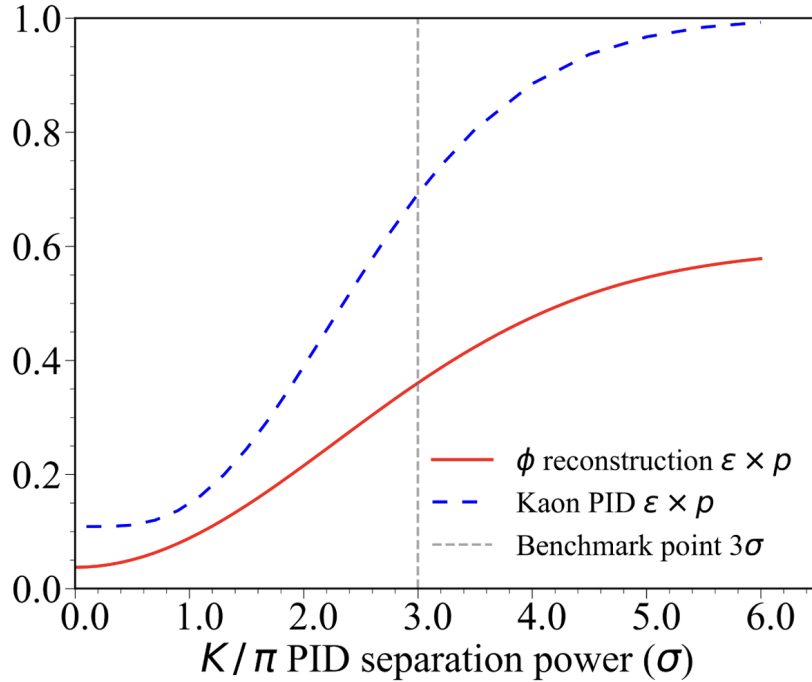


Charged Kaons from B/D hadrons → Flavor Physics

Charged Kaon from QCD → QCD

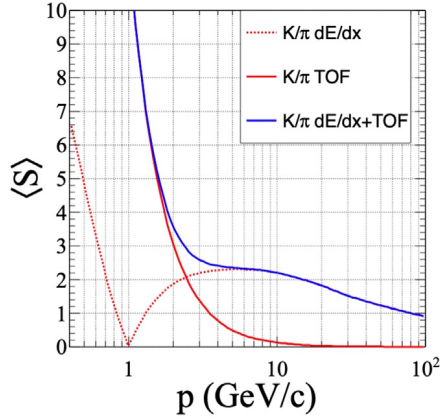
Both Contributed significantly to Jet Origin ID

Sep power < 3 sigma

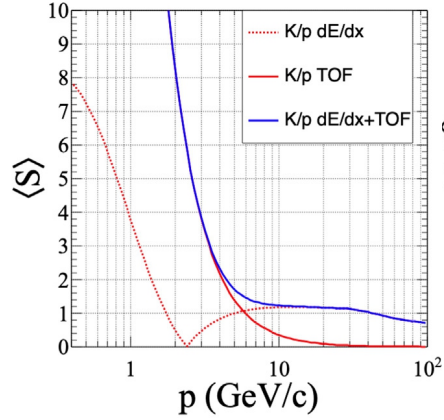


values $\mu_{K(\pi)}$ and corresponding standard deviations $\sigma_{K(\pi)}$.
The separation power is defined as $2|\mu_{\pi} - \mu_K|/(\sigma_{\pi} + \sigma_K)$.

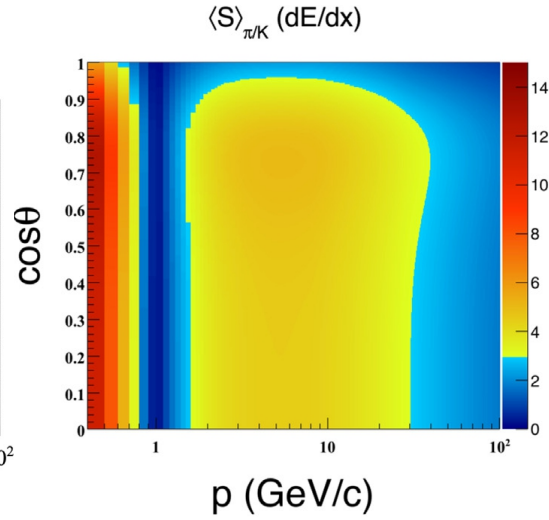
Sep. power



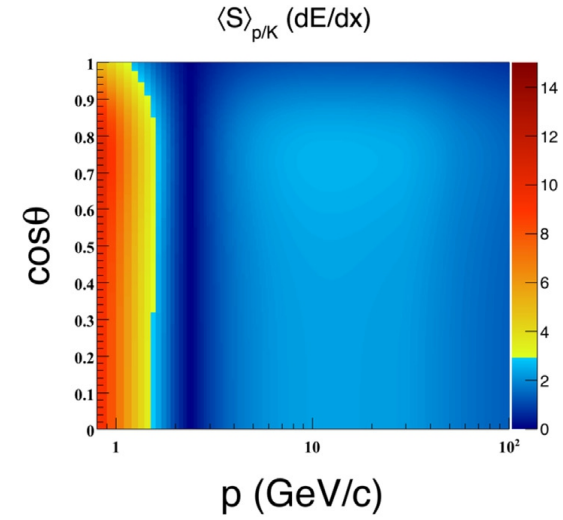
(a)



(b)

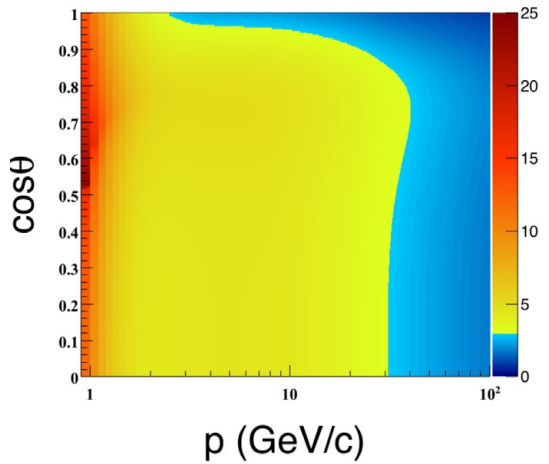


(a)



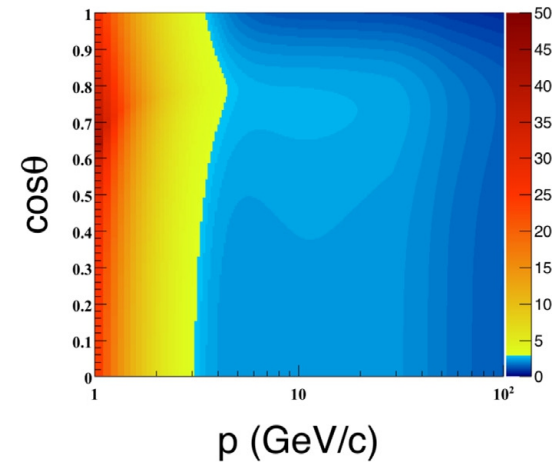
(b)

$\langle S \rangle_{\pi/K}$ (dE/dx + TOF)



(a)

$\langle S \rangle_{p/K}$ (dE/dx + TOF)



(b)

Table 3

The K^\pm identification performance with different factors, $\sigma_{actual} = factor \cdot \sigma_{intrinsic}$ with/without combination of TOF information at the Z-pole.

Factor		1.	1.2	1.5	2.
dE/dx	ϵ_K (%)	95.97	94.09	91.19	87.09
	pur_{K^+} (%)	81.56	78.17	71.85	61.28
dE/dx & TOF	ϵ_K (%)	98.43	97.41	95.52	92.3
	pur_{K^+} (%)	97.89	96.31	93.25	87.33

Requirement on dE/dx & dN/dx

Y. Zhu, S. Chen, H. Cui et al.

Nuclear Inst. and Methods in Physics Research, A 1047 (2023) 167835

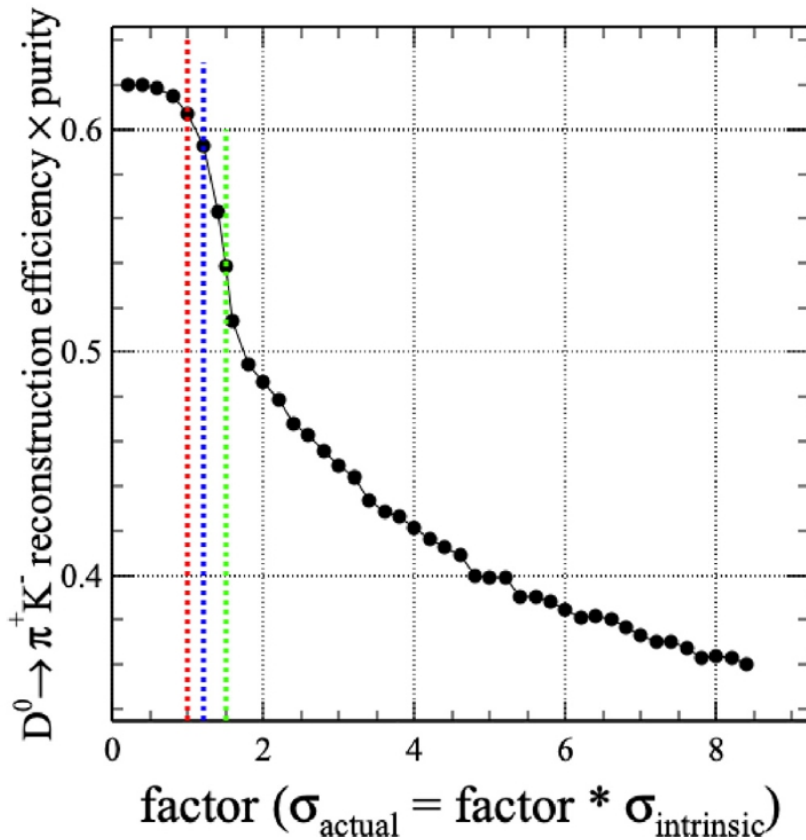


Fig. 12. The distribution of $D^0 \rightarrow \pi^+ K^-$ reconstruction performance as a function of the factor defined in $\sigma_{\text{actual}} = \text{factor} \cdot \sigma_{\text{intrinsic}}$. The red/blue/green line corresponds to the 0%/20%/50% degradation of dE/dx resolution.

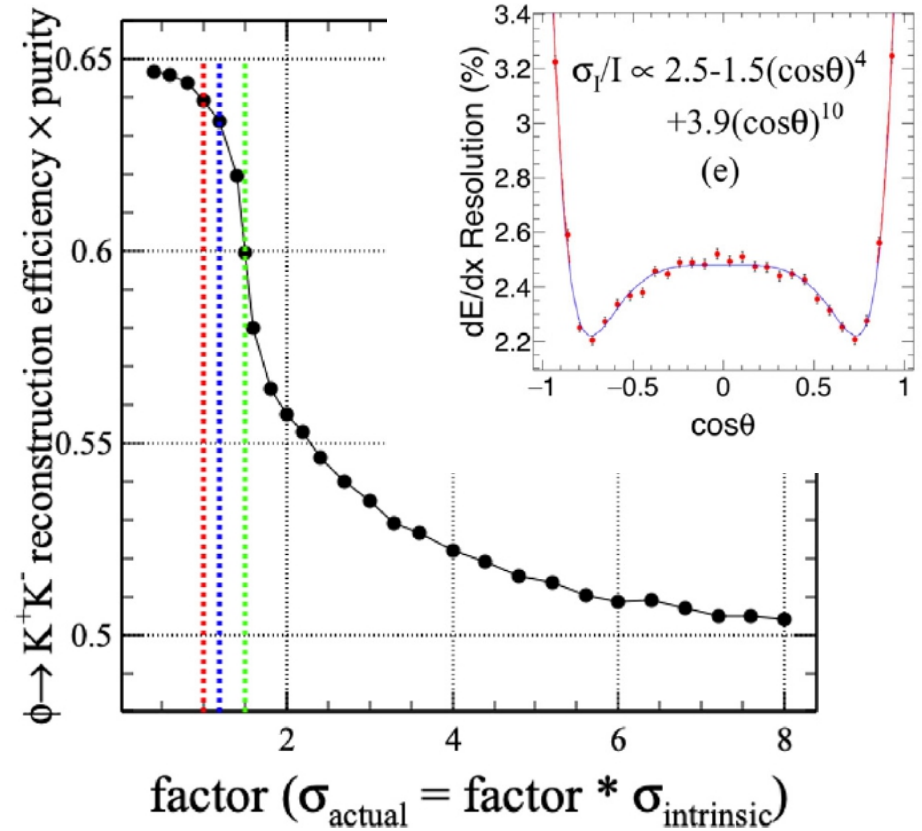
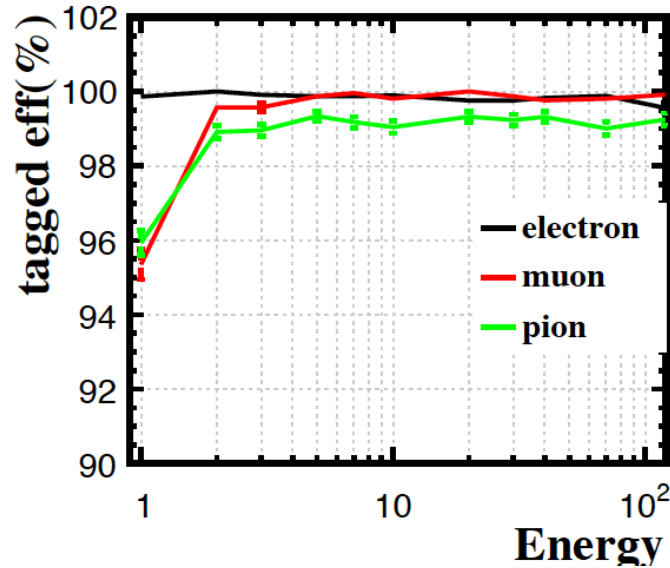
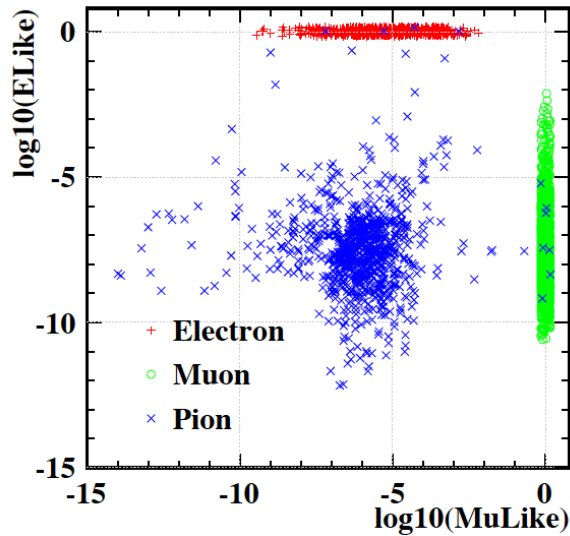


Fig. 13. The distribution of $\phi \rightarrow K^+ K^-$ reconstruction as a function of the factor defined in $\sigma_{\text{actual}} = \text{factor} \cdot \sigma_{\text{intrinsic}}$. The red/blue/green line corresponds to the 0%/20%/50% degradation of the dE/dx resolution.

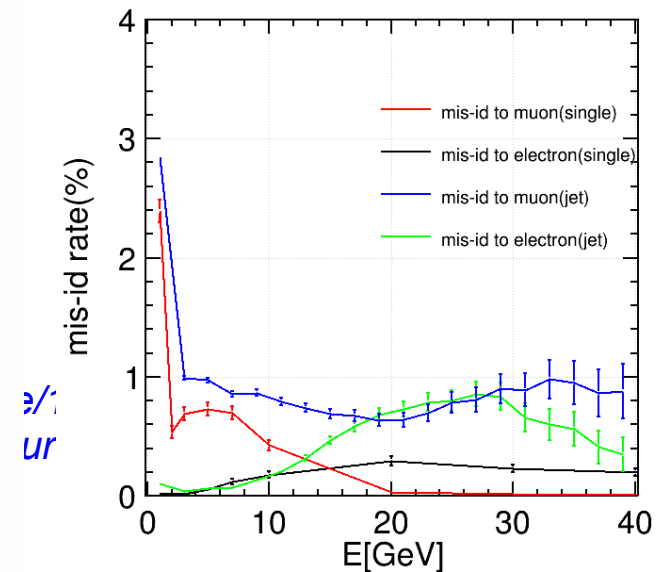
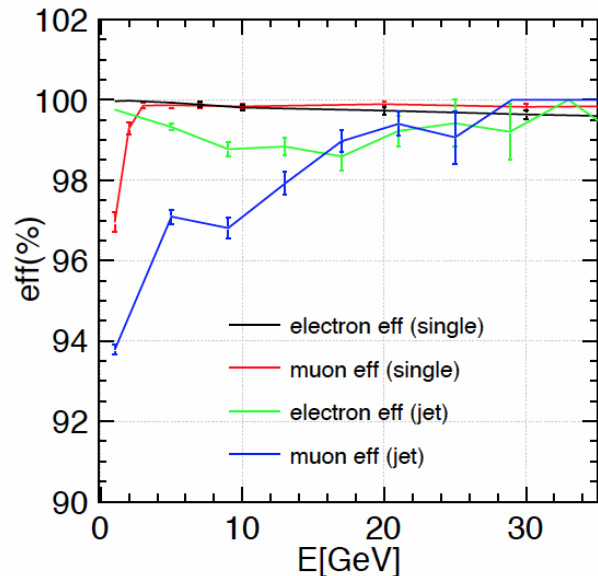
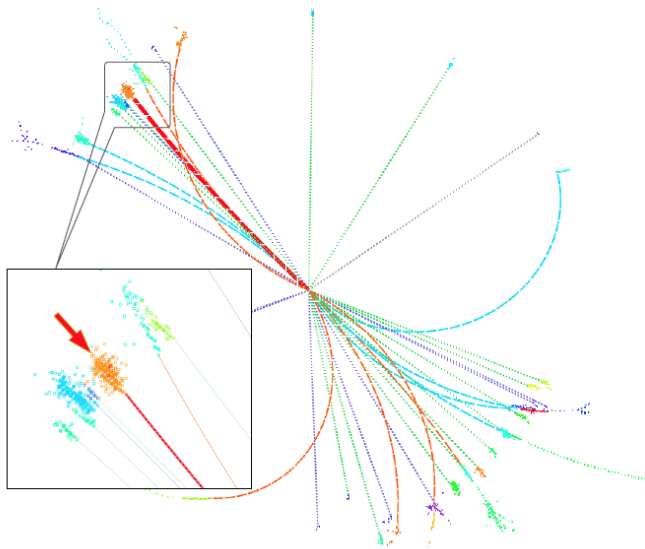
—► 3% dE/dx resolution in the barrel for $E > 2$ GeV tracks

Lepton: isolated & Inside jet



Isolated: for $E > 2$ GeV:
 lepton efficiency $> 99.5\%$ &&
 Pion mis id rate $\sim 1\%$

Inside Jet: percentage level
 degrading



Summary

- Physics Benchmarks selected, while new proposals are welcome
 - Based on existing study
 - Emphasize on Higgs (inc. Dark matter), and covers all observation channels.
- Corner stone performances
 - BMR: < 4% as a must... and shall pursue 3%
 - Jol: ~ baseline performance: b/c/s jet eff of 90/80/70% & charge flip rate of 10 - 20%
 - Pid: to identify all species of final state particles, inside jets, especially for charged Kaons.
- Sub-d performance:
 - Tracker dP/P ~ o(0.1%),
 - EM energy resolution ~ 3%/sqrt(E) \conv 0.3% ,
 - Had energy resolution ~ 50%/sqrt(E) \conv 2% .

Back up

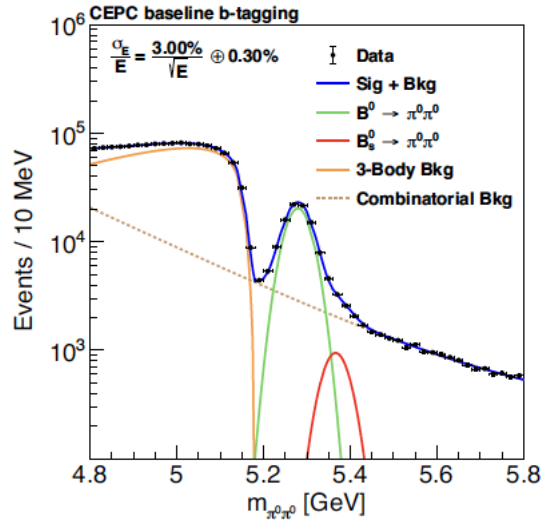


Figure 6. The reconstructed $m_{\pi^0\pi^0}$ distributions of $B^0 \rightarrow \pi^0\pi^0$, $B_s^0 \rightarrow \pi^0\pi^0$, and $Z \rightarrow q\bar{q}$ background after applying the baseline b -tagging and selections on energy and opening angle of π^0 pairs when the ECAL energy resolution is $\frac{3\%}{\sqrt{E}} \oplus 0.3\%$.

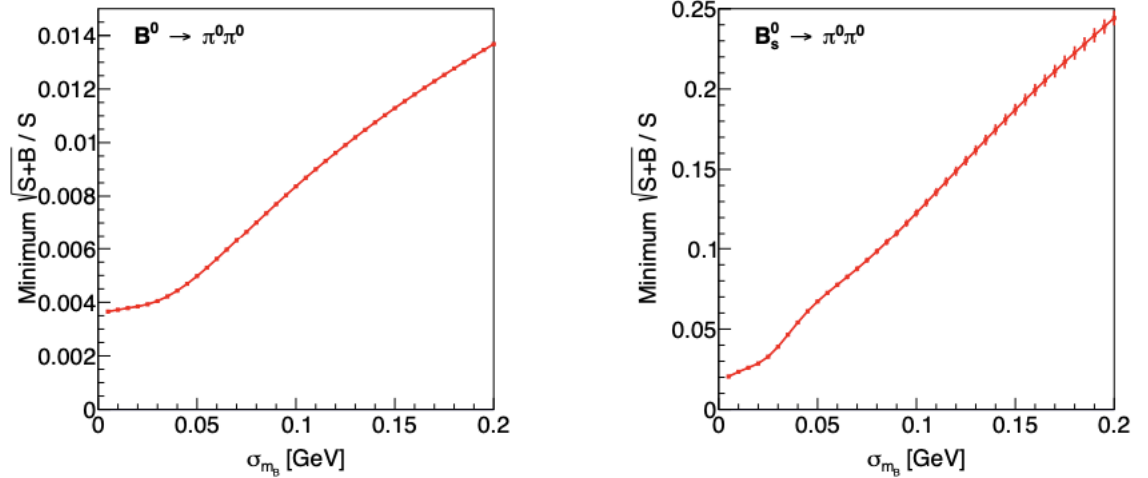


Figure 26: Relative statistical uncertainties of $\text{BR}(B^0 \rightarrow \pi^0\pi^0)$ (left) and $\text{BR}(B_s^0 \rightarrow \pi^0\pi^0)$ (right) versus B -meson mass resolution σ_{m_B} with four-photon final states. Plots taken from [32].

Charged fragment veto at Truth level

SiWECAL + GSHCAL (ideal parameter)

0: BMR ~3.32%, original

1: BMR ~2.98%, remove charged fragments

2: BMR ~2.73%, remove charged fragments + “Null MCP” event cut

PS: Two cases of “Null MCP” (fail to link to MCTruth Particle)

- PFO reconstructed by Energy Flow
- PFO caused by LumiCal Hits

